CARBON NANOTUBE MODIFIED GLASSY CARBON ELECTRODE FOR ELECTROCHEMICAL OXIDATION OF ALKYLPHENOL ETHOXYLATE

Short tittle: ELECTROCHEMICAL OXIDATION OF ALKYLPHENOL ETHOXYLATE BY CARBON NANOTUBEs

Yolanda Patiño[a], Eva Díaz[a], María Jesús Lobo-Castañón[b], Salvador Ordóñez[a]

[a]*Department of Chemical and Environmental Engineering,*

[b]*Department of Physical and Analytical Chemistry*

University of Oviedo, Faculty of Chemistry, Julián Clavería s/n, 33006 Oviedo, Spain

E-mail: diazfeva@uniovi.es

Abstract

The electrochemical oxidation of an emerging pollutant, 2-(4-methylphenoxy)ethanol (MPET), from water has been studied by cyclic voltammetry (CV). Multiwall carbon nanotubes glassy carbon electrodes (MWCNT-GCE) were used as working electrode due to their extraordinary electrochemical properties.

The oxidation process resulted irreversible, as just a single oxidation peak was obtained, and any reduction peaks was observed in the reverse scan. The electrocatalytic effect of MWCNT-GCE was confirmed since the oxidation peak increases in comparison to bare-GCE. The effect of functional groups on MWCNT was also studied with MWCNT-NH_2-GCE and MWCNT-COOH-GCE as working electrodes. The oxidation peak current follows the order MWCNT> MWCNT-NH_2> MWCNT-COOH. Taking into account the normalized peak current (I_p/A), MWCNT-NH_2 exhibits the best results due its strong interaction with MPET.

Under optimal conditions (pH=5.0 and V_{MWCNT}=10 µL), the degradation was studied for MWCNT-GCE and MWCNT-NH_2-GCE. A complete removal was obtained using MWCNT-GCE, for a volume/area (V/A) ratio equal to 19 after four CV cycles. In the case of MWCNT-NH_2-GCE, the maximum degradation was around 90% for V/A=37, higher than the obtained for MWCNT-GCE at the same conditions. In both cases, no organic by-products were detected, being the final total organic carbon removal close to 100 %.

Keywords: AOPs; cyclic voltammetry; emerging pollutants; endocrine disruptors

Introduction

Alkylphenol ethoxylates (APEs) are the main components of non-ionic surfactants, used to formulate products such as detergents, paints, plastic antioxidants, pesticides, wetting products, and petroleum recovery chemicals (Kuramitz et al., 2002), and considered an emerging organic pollutants group, with probed endocrine disrupting activity (Murray et al., 2017). Their extensive use in industrial and commercial formulations has resulted in an increase of their presence as common environmental pollutants found in sewage sludge and sediments, wastewater, surface waters, and even treated drinking (Kim et al., 2005; Nagarnaik et al., 2011). Besides, the degradation of this kind of pollutants in sewage treatment plants leads to the formation of more toxic and resistant metabolites, responsible for feminization and carcinogenesis on different organisms (Shao et al., 2003).

The European legislation by the Water Framework Directive 2000/60/EC includes some APEs in its priority list (European Commission, 2001). In addition, the European Directive No. 2003/53/EC has forbidden the use of nonylphenol and its ethoxylates in the European Union, but some industrial applications cannot replace them by alternative chemicals due to technical and economic reasons and continue using these compounds (Karci et al., 2014). Therefore, efficient methods for their removal must be developed.

Conventional treatments of water and effluents present difficulties to degrade APEs (Catapane et al., 2013) Thus, new technologies have been developed, such as advanced oxidation process (AOPs) and electrochemical degradation (Kuramitz et al., 2002; Kim et al., 2005). AOPs includes techniques like ozonation, photocatalysis, and Fenton, which employ a highly reactive oxidizing agent, such as hydroxyl radicals (HO·). Although AOPs are a good alternative and they are widely studied, they present some disadvantages: expensive process, excess consumption of chemicals and, in many cases, production of by-products of unknown effects, even more harmful than the starting products.

On the other hand, although the electrochemical degradation has been studied at lower extent than the abovementioned techniques, it presents several advantages, such as easiness of operation, the utilization of mild temperatures and pressures. At the same time, if the pollutant is oxidized, it can produce a complete mineralization of the target compound (Kim et al., 2005). All these facts make this technique as a good alternative for APEs degradation.

It is also necessary to take into account that these compounds are present in water at very low concentration, in the order of $\mu g \cdot L^{-1}$ to $ng \cdot L^{-1}$, which is a disadvantage for their removal (Esteban

et al., 2014), although the concentration can be increased through adsorption/desorption cycles (Patiño et al., 2017a).

Although the degradation should be carried out at constant potential, the application of a sweep potential is important in order to characterize the reaction and to obtain the best configuration for the different experimental variables. In this way cyclic voltammetry (CV) is commonly used to characterize redox systems, as well as to obtain information about the electrode transfer kinetics. Besides, CV has the advantage that with scanning the potential in both directions, it provides the opportunity to explore the electrochemical behaviour of species generated at the electrode (Settle et al., 1997).

Regarding to the working electrode, the electrochemical degradation can be improved with modified electrodes, which allow accelerating electron transfer for the electrochemical oxidation. Recently, multiwall carbon nanotube (MWCNT) are proposed for modifying electrodes due to their appropriate features - high surface area and porosity, enhanced electronic properties and rapid electrode kinetics – (Moyo et al., 2013). Besides, functionalized MWCNT can improve dispersion and generate chemical modifications on the electrode surface that can favour the degradation of certain species. The electrochemical degradation of nalidixic acid was studied in a previous work with non-functionalized and functionalized MWCNT-GCE (MWCNT-NH_2 and MWCNT-COOH) as working electrodes (Patiño et al., 2017b). The nalidixic acid was completely reduced to less toxic compounds using MWCNT-GCE as working electrode, which demonstrate the effectiveness of this technique. However, it is necessary to extend the study to other compounds with different electrochemical active functional groups to extend the effectiveness of electrochemical degradation.

For this reason, in this work, the electrochemical oxidation of 2-(4-methylphenoxy)ethanol, MPET, as representative of APEs has been studied by CV at MWCNT modified glassy carbon electrodes (MWCNT-GCE), and the influence of several variables such as pH, scan rate and amount of MWCNT have been studied. In order to determine the effect of functional groups on MWCNT, the electrochemical behaviour under two functionalized MWCNT – MWCNT-NH_2 and MWCNT-COOH – was compared with MWCNT under optimal conditions. In this way, the best working electrode for a complete degradation of MPET by a green technology could be selected.

Materials and Methods

Chemicals and reagents

2-(4-methylphenoxy)ethanol (MPET) was purchased from TCI Europe N.V., with a purity > 98% and used in the experiments directly without any further purification.

The chemicals employed for the phosphate buffer (PBS) (NaCl, KCl, KH_2PO_4 and Na_2HPO_4), $K_4[Fe(CN)_6]$ and $K_3[Fe(CN)_6]$ were obtained from Sigma-Aldrich.

Three different commercial multi-walled carbon nanotubes manufactures by Dropsense (MWCNT, MWCNT-NH_2 and MWCNT-COOH) were tested in this work.

Instrumentation

Cyclic voltammetry, were performed using a Zahner XPOT Potentiostat. The surface areas of the working electrodes were performed using a µ-Autolab Potentiostat/Galvanostat PGSTAT20.

Batch oxidation was performed in an undivided electrolytic cell with a conventional three electrodes arrangement: bare or modified glassy carbon (GCE) as working electrode, saturated calomel (SCE) as reference electrode and platinum (Pt) as auxiliary electrode. Before each measure, the solution was deoxygenated by passing purified nitrogen gas for 20 min, which prevents any interference from oxygen signals. Besides, prior to each analysis a blank was performed analyzing the buffer without MPET, to ensure that once the compound was added, the response obtained was only relative to MPET.

MPET and the by-products obtained after electrochemical degradation were quantified by GC-MS in a Shimadzu GC/MS QP2010 Plus instrument, using a 30 m long TRB-5MS capillary column by prior extraction in chloroform using a volume ratio (1:1) which allows to determine concentrations of order of ppb. Likewise, the MPET degradation was confirmed by total organic carbon (TOC) measurements, which were performed using a TOC analyser (Shimadzu TOC-VCSH).

Preparation of the modified electrodes

Suspensions of MWCNTs were prepared by dispersing into dimethylformamide (DMF) (0.25 $g \cdot L^{-1}$) using ultrasonication until obtain a well-dispersed suspension (García-González et al., 2013).

The bare-GCE was polished successively with 0.3 and 0.05 µm alumina slurries, and washed by ultrasonication in double distilled deionized water. After the electrode was dried in the air, it was dropped by depositing 5, 10 or 15 µL of the MWCNTs suspension on the working area and then dried under room temperature before electrochemical measurements.

Results and Discussion

Surface area electrode study

Before starting the experiments, it is necessary to determine the active surface areas. They were obtained by cyclic voltammetry (CV) using 1mM $K_3[Fe(CN)_6]$ solution in PBS buffer at different scan rates. According to Randles-Sevcik equation, which relates the peak current (I_p) to scan rate potential (ν) at 20°C for an electrochemically reversible process (Eq. 1)

$$i_p = 2.69 \times 10^5 \, n^{3/2} \, A \, C_0 \, {D_R}^{1/2} \, \nu^{1/2} \quad (1)$$

Where i_p is the peak current, n is the number of electron transfer (n=1), A is the surface area of the electrode, C_0 is the concentration of species being oxidised, D_R is the diffusion coefficient (D_R= 7.6 x 10^{-6} cm^2s^{-1}) and ν is the scan rate; the electrochemically active area can be estimated from the slope of i_p *vs* $\nu^{1/2}$.

The electrode surface areas obtained follow the order: MWCNT (0.135 cm^2) > MWCNT-NH_2 (0.054 cm^2) > MWCNT-COOH (0.051 cm^2) > Bare (0.040cm^2).

The electrochemical effective surface area increases after modification of GCE. This increase is less pronounced for MWCNT-COOH and MWCNT-NH_2. However, for MWCNT the effective surface area increases more than three times compared with the bare electrode, and more than twice for functionalized MWCNT. These differences were attributed in a previous work (Patiño et al., 2017b) to the more uniform surface with several carbon nanotubes layers and high film thickness (0.9 μm) of the MWCNT, whereas functionalized materials present lower density of carbon nanotubes.

There is also consensus in the literature about the modification of the electrode surface area after the deposition of the carbon nanotubes, being in all cases the final area after modification higher than for bare-GCE (d et al., 2011; Dogan-Topal et al., 2013).

Electrochemical behaviour of MPET on GCE and MWCNT modified electrode

The cyclic voltammogram of $1 \cdot 10^{-5}$ M MPET on bare-GCE and MWCNT-GCE at pH 5 in PBS buffer solution is shown in Fig. 1. As can be seen in the figure, the oxidation process of MPET was irreversible for both electrodes, since no peak was observed in the reverse scan. Oxidation peaks were observed at 1.28 and 1.31, for bare-GCE and MWCNT-GCE, respectively. It is observed that the peak current increases at MWCNT-GCE which may be indicative of the catalytic effect of MWCNT on the electrochemical oxidation of MPET (Jain and Rather, 2011; Jain and Sharma, 2012). The reason of this improvement with MWCNT is usually attributed to their electronic structure and the higher effective area of the electrode. Taking into account the density current (peak current/electrode area), the maximum value is also obtained for MWCNT, indicating that

the effective surface area is not the only parameter determining the electrochemical response (Fig. 1b). The high electrical conductivity of carbon nanotubes accelerates the electron transfer reaction rate in the oxidation process (Gupta et al., 2013). Similar behaviour was also observed by other authors using multiwall carbon nanotubes modified glassy carbon electrode as working electrode (Fotouhi and Alahyari, 2010; Gupta et al., 2013).

Once the influence of MWCNT on the MPET oxidation was demonstrated, it is important to determine the optimum amount of MWCNT to drop on the electrode, since it can modify the properties and functions of the surface electrode. For this reason, different volumes – 5, 10 and 15 µL – of the MWCNT suspension were dropped, and the peak current was compared (Fig.2). The oxidation peak current increases with increases in the amount of MWCNT up to 10 µL, volume from which the peak current decreases. The peak current variation is related to the thickness of the film. If the film is too thin, the amount of MPET adsorbed on the electrode surface is small, which involves a small peak current. Contrary, when it is too thick, film conductivity gets reduced, making the film less stable and MWCNTs could leave off the electrode surface easily (Jain and Rather, 2011; Patil et al., 2011). Besides, the thick electrode hinders the conductivity through the whole film, decreasing in this way the ability of the molecule to be adsorbed and, hence, to be degraded what is showed in a slower peak current (Fotouhi and Alahyari, 2010; Jain and Sharma, 2012; Dogan-Topal et al., 2013). Therefore, 10 µL was selected as the optimum amount of MWCNT suspension.

The effect of the concentration on the voltammogram is shown in Fig. 3, where the peak current obtained using MWCNT-GCE increases with MPET concentration. Although the response is close to linearity, it cannot be considered linear with a correlation coefficient of r^2=0.9784.

Optimization of parameters

Cyclic voltammograms on MWCNT-GCE of $1 \cdot 10^{-5}$ M MPET at different scan rates of 10 to 50 mVs^{-1} were done in order to investigate the effect of this parameter. By increasing the scan rate, the peak current increases and also, peak potential shifted toward more positive values, typical effect with increasing scan rate (Fotouhi and Alahyari, 2010; Patil et al., 2011; Dogan-Topal et al., 2013).

Scan rate studies provide information about whether the process is controlled by diffusion or adsorption. It was found that the logarithm of peak current is linear to the logarithm of scan rate, according to the equation (2). If the slope is 0.5, the process is under diffusion controlled, but contrary, when the slope is 1.0, the process is controlled by (Dogan-Topal et al., 2013). In

this case, the slope has an intermediate value, which suggests a mixed control: diffusion-adsorption (Grosser, 1993).

$$\ln I_p = 0.7608 \ln v + 0.387 \quad (r^2 = 0.991) \qquad (2)$$

A positive shift in Ep was also observed with increase in scan rate, which confirms the irreversible nature of the catalytic oxidation of MPET (Moyo et al., 2013). Likewise, the electrochemical behaviour is also affected by the pH of the supporting electrolyte. The voltammetric oxidation of MPET was studied in the pH range of 3 to 9. As shown in Fig. 4 the oxidation peak current reaches a maximum in current at pH 5, after that it decreases. Considering this pH effect, pH of 5 was chosen for the rest of experiments.

The relationship between the oxidation potential and pH is also represented in Fig. 4. It was found that the peak potential shifted towards negative potentials with increasing pH, which indicates that protons are directly involved in the oxidation of MPET (Zheng et al., 2012). The oxidation peak potential increases linearly with the pH, and the linear regression equation is:

$$E_p\ (V) = 0.0515\ pH + 1.5865 \quad (r^2 = 0.995) \qquad (3)$$

The slope is close to the theoretical Nernstian value (0.059 V), indicating the participation of the same protons and electrons during the oxidation reaction (Łuczak, 2008).

Effect of functional groups of MWCNT

The effect of the functionalization of MWCNT on the electrochemical oxidation of MPET, has been studied by CV using three different modified MWCNT-GCE as working electrodes: MWCNT, MWCNT-NH_2 and MWCNT-COOH. The behaviour is different for each working electrode, which can be seen from Fig. 5. The peak current increases in the order: MWCNT > MWCNT-NH_2 > MWCNT-COOH, coincident with the increase in the electrode surface area (Fig 5a). However in the case of functionalized MWCNT, where the effective area is very similar, there are major differences in the peak intensity obtained, suggesting that other factor influences the oxidation process. It was demonstrated that the process presents mixed control: diffusion-adsorption. During the electrochemical process, MPET is adsorbed on the electrode surface, where the electrochemical oxidation takes places, so the peak current trend may be affected also by the different strength of the adsorption due to the functionalization of MWCNT. The adsorption of MPET onto MWCNT and functionalized MWCNT was studied in a previous work, by batch

adsorption at three different temperatures (298, 303 and 308 K) (Patiño et al., 2015). The strength of the interaction was measured in terms of standard enthalpy (ΔH°, $kJ \cdot mol^{-1}$) and follows the order MWCNT-NH_2 (101.7) > MWCNT (88.1) > MWCNT-COOH (67.4). In order to take into account the differences in active area of the selected electrodes, and with the aim to determine if the adsorption influences the electrochemical oxidation, the density current (I_p/A, measured in $\mu A/cm^2$) has been calculated and its evolution with the pH represented (Fig. 5b). The density current decreases in the order: MWCNT-NH_2 > MWCNT > MWCNT-COOH, which is coincident with the strength of the interaction (Patiño et al., 2015) (Fig. 6). As the strength of interaction increases, the stability of the MPET adsorbed increases, decreasing the trend to leave the electrode surface. Thus, a higher strength implies a higher normalized peak current.

Besides, MWCNT-NH_2 presents the highest normalized peak current, since the nitrogen content in MWCNT could increase its affinity for MPET. In this case, the electronic interactions play a key role, where the nitrogen present on the MWCNT acts as electron donor and the aromatic ring of MPET as electron receptor, promoting the adsorption of the pollutant on the electrode surface (Fan et al., 2011; Patiño et al., 2015).

On the contrary, there is no a relationship regarding to the effect of the surface chemistry. The electrode surface is negatively charged, since working at pH=5, it is in all cases higher than the pH_{PZC} of the multiwall carbon nanotubes - pH_{PZC} (MWCNT)=4.19, pH_{PZC} (MWCNT-NH2)=4.70 and pH_{PZC} (MWCNT-COOH)=0.64 – (Patiño et al., 2015). On the other hand, MPET is expected to be in the protonated form (pKa≈14), acquiring positive charge. Therefore, MWCNT-COOH should present the best behaviour if the effect of the surface chemistry plays an important role, since it presents the most negative surface (pH_{PZC}=0.64), which is contrary to the results obtained (Patiño et al., 2015).

Removal of MPET using MWCNT-GCE and MWCNT-NH_2-GCE electrodes

MPET degradation has been studied by CV using two different working electrodes. Although MWCNT-NH_2 presents the highest density current, it must be taken into account that many times the electrode surface is a limiting factor. Therefore both, the effect of area and strength of interaction, should be considered. For this reason, MWCNT and MWCNT-NH_2 modified GCE have been tested as electrodes.

Both working electrodes were tested by CV using a potential range of 0.9 to 1.7 V for an initial concentration of $1 \cdot 10^{-5}$ M. The final concentration and possible intermediates were analysed by GC-MS with the aim to estimate the percentage of degradation.

The surface area of the electrodes is a constant parameter after modification, so it is necessary to obtain the total volume to be treated for which the maximum degradation is obtained. In this way, the optimum volume/area (V/A) ratio will be obtained.

The oxidation of MPET was carried out initially in a total volume of 5 mL for both working electrodes: MWCNT (V/A=37) and MWCNT-NH_2 (V/A=98) modified GCE. After one CV, the degradation of MPET was lower than 31% for both working electrodes, so several cycles of CV were performed in order to degrade a new fraction of the pollutant at each new cycle, increasing the percentage of degradation (Fig. 7 empty symbols). With each new CV cycle, a new amount of MPET is adsorbed on the electrode surface and therefore oxidized on the electrode surface. The maximum degradation obtained was 79 and 58% for MWCNT and MWCNT-NH_2 respectively (between 2.6 and 2.8 times greater than for one CV), keeping it constant after four CV cycles.

Since it is not possible to increase the MPET degradation by more CV cycles, the next strategy proposed to get this purpose was to decrease the total volume to be treated. In this way, the volume/area (V/A) ratio was modified in order to obtain a higher degradation (Fig. 7 full symbols). For MWCNT modified GCE, the degradation was carried out for a total volume of 2.5 mL (V/A=19) and for one to five cyclic voltammograms. In this case, the degradation obtained after one CV is more than double compared to a total volume of 5 mL, and a total degradation was achieved after four CV. In the case of MWCNT-NH_2 modified GCE, the total volume was decreased to 1.9 mL (V/A=37.3), because it is the smallest volume that supports the experimental device and it is coincident with the first V/A ratio employed for MWCNT. In this case the maximum degradation is around 85 - 90% and more or less constant after three CV. For this working electrode it was no possible to reach a complete degradation due to the experimental constraints.

When the V/A ratio is the same for both electrodes, the degradation is a bit higher for MWCNT-NH_2-GCE than for MWCNT-GCE, which is due to the high interaction strength. The MPET adsorbed on the electrode surface is more stable in this case, making it more difficult to leave the electrode surface during the degradation process. However, when the volume to be treated is a limiting factor, MWCNT-GCE provides better results. The results provide a new pathway for the electrochemical degradation of these kind of pollutants and the degradation can be performed at constant potential, higher than the peak potential (1.31 V). Kuramitz et al. (2002) studied the electrochemical removal of p-nonylphenol at constant potential with a carbon fibre electrode as working electrode with a removal efficiency of 100%. Besides, the results obtained by electrochemical degradation, can be compared with those obtained by other authors using advanced oxidation processes (AOPs). Nagarnaik et al. (2011) studied the degradation of APEs

by UH – UV/H_2O_2, FH – Fe/H_2O_2, UFH – $Fe/UV/H_2O_2$. The maximum removal efficiency follows the order: UH – UV/H_2O_2 (97.1%) > UFH – $Fe/UV/H_2O_2$ (85.8%) > FH – Fe/H_2O_2 (95.5%) with values lower or similar than the obtained in the present work. Karci et al. (2014) studied the oxidation of an nonionic surfactant (NP-10) by three AOPs, whose oxidation efficiency decreases in the order: UV/H_2O_2 (100%) > Photo-Fenton (100%) > Fenton (20%). Although in some cases, a total oxidation could be obtained by AOPs, electrochemical oxidation provides a low cost and clean technology.

The final concentration and sub-products formation was analysed by GC-MS after each test, observing an important diminution of the MPET after the electrochemical degradation, which confirms that oxidation takes place. Likewise, any other compound was detected, which suggests that MPET is completely removed from the aqueous sample. In order to confirm the absence of MPET and other organic compounds in the final solution, Fig. 8 shows the evolution of the total organic carbon (TOC) with each new cycle. The analysis were carried out for MWCNT and MWCNT-NH_2 under conditions where maximum degradation was reached. TOC removal reaches values of which also confirms the best behaviour of MWCNT for MPET degradation.

Conclusions

The results obtained offer an alternative for the degradation of MPET from water by cyclic voltammetry.

MWCNT modified GCE exhibits an electrocatalytic effect on the electrochemical oxidation of MPET, with a peak intensity four times higher than bare-GCE.

Different parameters were optimized in order to obtain an improved oxidation: carbon nanotube loading (10 µL of CNTs suspension), the pH (5.0) and the scan rate (50 $mV \cdot s^{-1}$).

Functionalized MWCNT were checked in order to determine how the functional groups on MWCNT affect to the electrochemical oxidation process. The peak current (Ip) increases in the order: MWCNT > MWCNT-NH_2 > MWCNT-COOH, coincident with the electrode surface area. The order for the density current (I_p/A) changes: MWCNT-NH_2 > MWCNT > MWCNT-COOH. This trend is coincident with the strength of adsorption on the electrode surface and in addition, the nitrogen presents on MWCNT-NH_2 increases the affinity for MPET through electronic interaction.

The MPET was removed with MWCNT-GCE after four CV cycles under optimal conditions and V/A ratio equal to 19. In the case of MWCNT-NH_2 the maximum degradation obtained was around 90% for a V/A = 37. Degradation was confirmed by TOC measurements, reaching a reduction between 93 and 99 % after the four CV cycles, as well as by GC-MS analysis of the

treated samples, where no by-products were observed. Therefore, the MPET adsorbed on the electrode surface in each CV cycle is oxidized, allowing a new amount of compound to be deposited and oxidized. This way provides a green methodology without producing more toxic compounds.

Acknowledgements

This work was supported by the Spanish Government (contract CTQ2011-29272-C04-02) and by the Government of the Principalty of Asturias (contract FC-15-GRUPIN14-078). Y. Patiño acknowledges the Government of the Principality of Asturias for a Ph.D. fellowship (Severo Ochoa Program).

References

Catapane M., Nicolucci,C., Menale C., Mita L., Rossi S., Mita D.G. & Diano, N. 2013 Enzymatic removal of estrogenic activity of nonylphenol and octylphenol aqueous solutions by immobilized laccase from Trametes versicolor. *J. Hazard Mat*. **248–249**, 337-346.

Dogan-Topal B., Bozal-Palabıyık B., Uslu B. & Ozkan S.A. 2013 Multi-walled carbon nanotube modified glassy carbon electrode as a voltammetric nanosensor for the sensitive determination of anti-viral drug valganciclovir in pharmaceuticals. *Sens. Actuators B: Chem*. **177**, 841-847.

European Commision, Decision No. 2455/2001/EC of the European Parliament and of the Council of 20 November 2001 establishing the list of priority substances in the field of water policy and amending Directive 2000/60/EC, Official Journal of the EC, L331, 15.12.2001

Esteban S., Gorga M., Petrovic M., González-Alonso S., Barceló D. & Valcárcel Y. , 2014 Analysis and occurrence of endocrine-disrupting compounds and estrogenic activity in the surface waters of Central Spain. *Sci. Total Environ*. **466–467**, 939-951.

Fan J., Yang W. & Li A. 2011 Adsorption of phenol, bisphenol A and nonylphenol ethoxylates onto hypercrosslinked and aminated adsorbents. *React. Funct. Polym*. **71**(10), 994-1000.

360 Fotouhi L. & Alahyari M. 2010 Electrochemical behavior and analytical application of
361 ciprofloxacin using a multi-walled nanotube composite film-glassy carbon electrode. *Colloids*
362 *Surf. B: Biointerfaces* **81** (1), 110-114.

363 García-González R., Fernández-La Villa A., Costa-García A. & Fernández-Abedul M.T. 2013
364 Dispersion studies of carboxyl, amine and thiol-functionalized carbon nanotubes for improving
365 the electrochemical behavior of screen printed electrodes. *Sens. Actuators B: Chemical* **181**, 353-
366 360.

367 Gupta V.K., Jain A.K. & Shoora S.K. 2013 Multiwall carbon nanotube modified glassy carbon
368 electrode as voltammetric sensor for the simultaneous determination of ascorbic acid and
369 caffeine. *Electrochim. Acta* **93**, 248-253.

370 Jain R. & Rather J.A. 2011 Voltammetric determination of antibacterial drug gemifloxacin in
371 solubilized systems at multi-walled carbon nanotubes modified glassy carbon electrode. *Colloids*
372 *Surf. B: Biointerfaces* **83** (2), 340-346.

373 Jain R. & Sharma S. 2012 Glassy carbon electrode modified with multi-walled carbon nanotubes
374 sensor for the quantification of antihistamine drug pheniramine in solubilized systems. *J. Pharm.*
375 *Anal*. **2** (1), 56-61.

376 Gosser Jr D.K. 1993. Cyclic Voltammetry, Simulation and Analysis of Reaction Mechanisms, New
377 York.

378 Karci A., Arslan-Alaton I., Bekbolet M., Ozhan G. & Alpertunga B. 2014 H_2O_2/UV-C and Photo-
379 Fenton treatment of a nonylphenol polyethoxylate in synthetic freshwater: Follow-up of
380 degradation products, acute toxicity and genotoxicity. *Chem. Eng. J*. **241**, 43-51.

381 Kim J., Korshin G.V. & Velichenko A.B. 2005 Comparative study of electrochemical degradation
382 and ozonation of nonylphenol. *Water Res*. **39** (12), 2527-2534.

383 Kuramitz H., Saitoh J., Hattori T. & Tanaka S. 2002 Electrochemical removal of p- nonylphenol
384 from dilute solutions using a carbon fiber anode. *Water Res*. **36** (13), 3323-3329.

385 Łuczak T. 2008 Preparation and characterization of the dopamine film electrochemically
386 deposited on a gold template and its applications for dopamine sensing in aqueous solution.
387 *Electrochim. Acta* **53** (19), 5725-5731.

388 Moyo M., Okonkwo J.O. & Agyei N.M. 2013 A Novel Hydrogen Peroxide Biosensor Based on
389 Adsorption of Horseradish Peroxidase onto a Nanobiomaterial Composite Modified Glassy
390 Carbon Electrode. *Electroanalysis* **25** (8), 1946-1954.

391 Murray A., Örmeci B. & Lai E.P.C. 2017 Use of sub-micron sized resin particles for removal of
392 endocrine disrupting compounds and pharmaceuticals from water and wastewater. *J. Environm.*
393 *Sci*. **51**, 256-264.

394 Nagarnaik P.M. & Boulanger B., 2011 Advanced oxidation of alkylphenol ethoxylates in aqueous
395 systems. *Chemosphere* **85** (5), 854-860.

396 Patil R.H., Hegde R.N. & Nandibewoor S.T. 2011 Electro-oxidation and determination of
397 antihistamine drug, cetirizine dihydrochloride at glassy carbon electrode modified with multi-
398 walled carbon nanotubes*. Colloids Surf. B: Biointerfaces* **83** (1), 133-138.

399 Patiño Y., Díaz E., Ordóñez S., Gallegos-Suarez E., Guerrero-Ruiz A. & Rodríguez-Ramos I. 2015
400 Adsorption of emerging pollutants on functionalized multiwall carbon nanotubes. *Chemosphere*
401 **136**, 174-180.

402 Patiño Y., Díaz E. & Ordóñez S. 2017a Micropollutants pre-concentration using adsorption–
403 desorption cycles: application to chlorinated paraffins and alkyl-phenol derivatives. *J. Chem.*
404 *Technol. Biotechnol.* **92** (5), 1076-1084.

405 Patiño Y., Pilehvar S., Díaz E., Ordóñez S. & De Wael K. 2017b Electrochemical reduction of
406 nalidixic acid at glassy carbon electrode modified with multi-walled carbon nanotubes. *J Hazard*
407 *Mat*. **323**, 621-631.

408 Settle F.A. 1997. Handbook of instrumental techniques for analytical chemistry. Upper Saddle
409 River, NJ : Prentice Hall PTR.

410 Shao B., Hu J., & Yang M. 2003 Nonylphenol Ethoxylates and Their Biodegradation Intermediates
411 in Water and Sludge of a Sewage Treatment Plant. Bull Environ. *Contam. Toxicol*. **70** (3), 0527-
412 0532.

413 Zheng Q., Yang P., Xu H., Liu J. & Jin L. 2012 A simple and sensitive method for the determination
414 of 4-n-octylphenol based on multi-walled carbon nanotubes modified glassy carbon electrode.
415 *J. Environ. Sci.* **24** (9), 1717-1722.
416

FIGURE CAPTIONS

Figure 1. Electrochemical oxidation of 1×10^{-5} M MPET (CV, scan rate 50 mVs^{-1}) over the bare GCE electrode (- - -), and MWCNT-GCE (—). Background electrolyte signal is also displayed (....), represented as peak current *vs* potential (SCE) (a) and density current *vs* potential (SCE) (b).

Figure 2. Effect of accumulation volumes of MWCNT on peak current response of $1\cdot10^{-5}$ M MPET.

Figure 3. Voltammograms obtained with MWCNT-GCE (CV, scan rate 50 mVs^{-1}) for different MPET concentration: (a) $1\cdot10^{-5}$, (b) $3\cdot10^{-5}$, (c) $6\cdot10^{-5}$, (d) $9\cdot10^{-5}$ and (e) $1.2\cdot10^{-4}$. Represented as peak current *vs* potential (SCE).

Figure 4. Dependence of oxidation peak current (●) and oxidation peak potential (□), as a function of pH by cyclic voltammetry on MWCNT-GCE (1×10^{-5} M MPET and scan rate: 50 mVs^{-1})

Figure 5. Effect of functionalized MWCNT on the electro-oxidation of MPET by CV (pH 5 and scan rate 50 mVs^{-1}): MWCNT-GCE (—), MWCNT-NH_2-GCE (---),MWCNT-COOH-GCE (-·-·) and Bare-GCE (– –) as working electrodes. Represented as peak current *vs* potential (SCE) (a) and density current *vs* potential (SCE) (b)

Figure 6. Influence of the enthalpy of adsorption ($kJ\cdot mol^{-1}$) in the ratio (I_p/A) for electro-oxidation of MPET by CV under three different working electrodes: MWCNT-GCE, MWCNT-NH_2-GCE and MWCNT-COOH-GCE (pH 5 and scan rate 50 mVs^{-1}).

Figure 7. Degradation of MPET by CV (pH 5 and scan rate 50 mVs^{-1}) under different working electrodes and V/A ratio: (●) MWCNT-GCE, VT/A = 19, (○) MWCNT-GCE, VT/A = 37, (□) MWCNT-NH_2-GCE, VT/A = 98, (■) MWCNT-NH_2-GCE, VT/A = 37

Figure 8. Evolution of TOC under different CV cycles for MWCT at V_T/A=19 (solid blue bar) and MWCNT-NH_2 at V_T/A=37 (striped yellow bar)

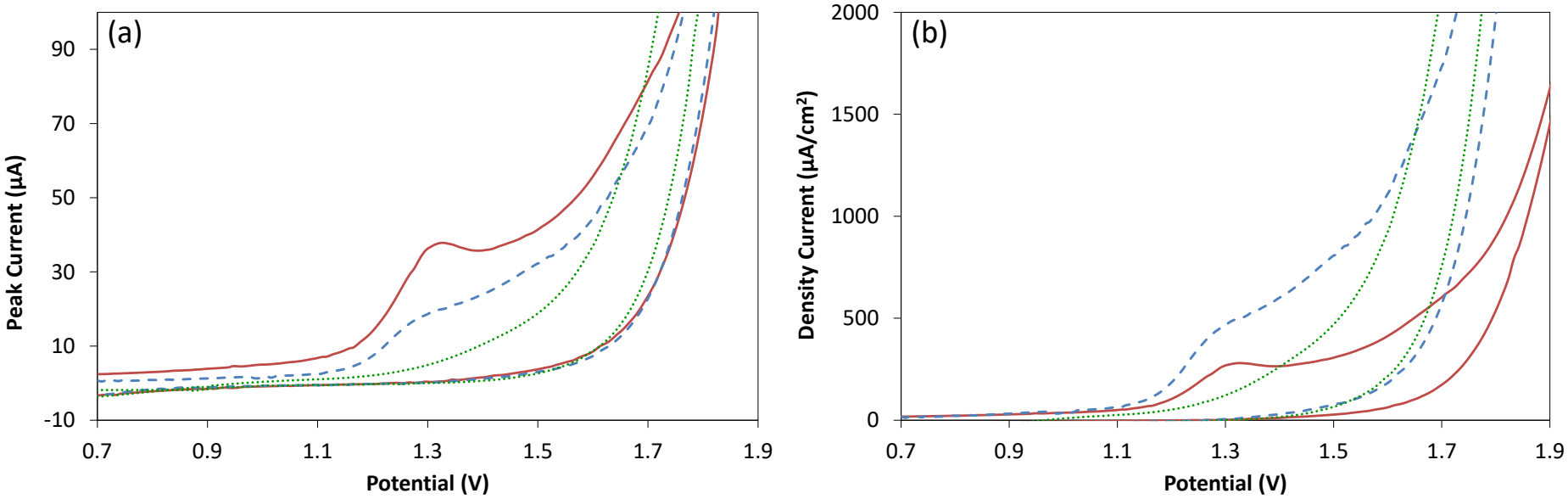
(a)
Peak Current (µA)
90
70
50
30
10
-10
0.7
0.9
1.1
1.3
1.5
1.7
1.9
Potential (V)
(b)
Density Current (µA/cm²)
2000
1500
1000
500
0
0.7
0.9
1.1
1.3
1.5
1.7
1.9
Potential (V)

Figure 1

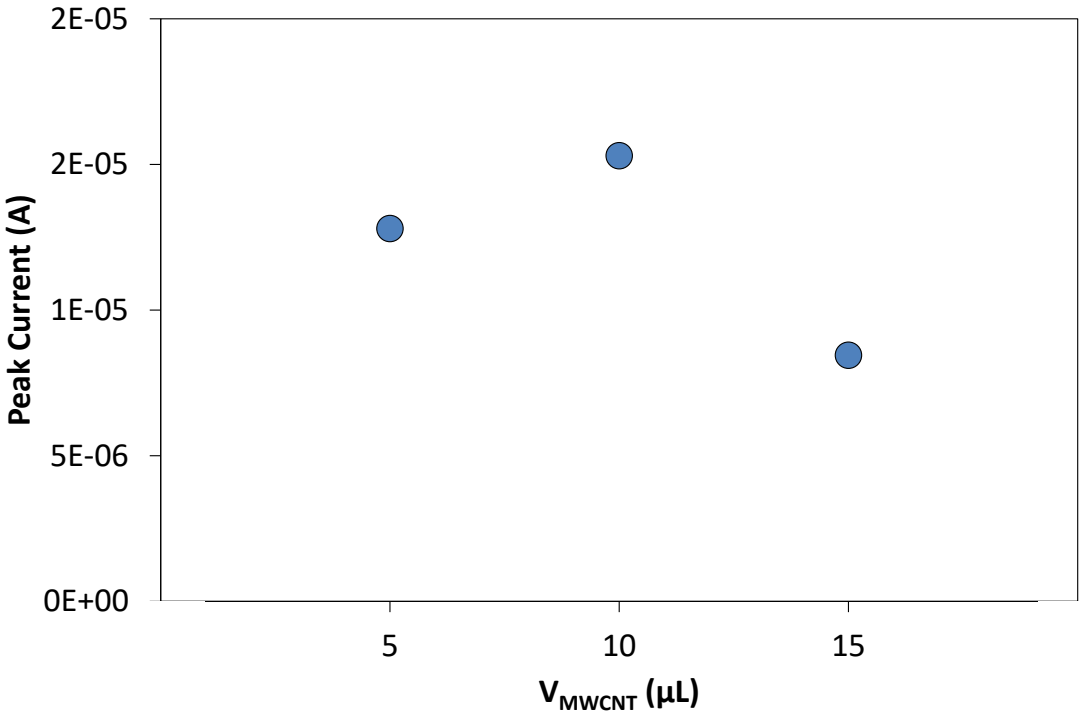

Figure 2

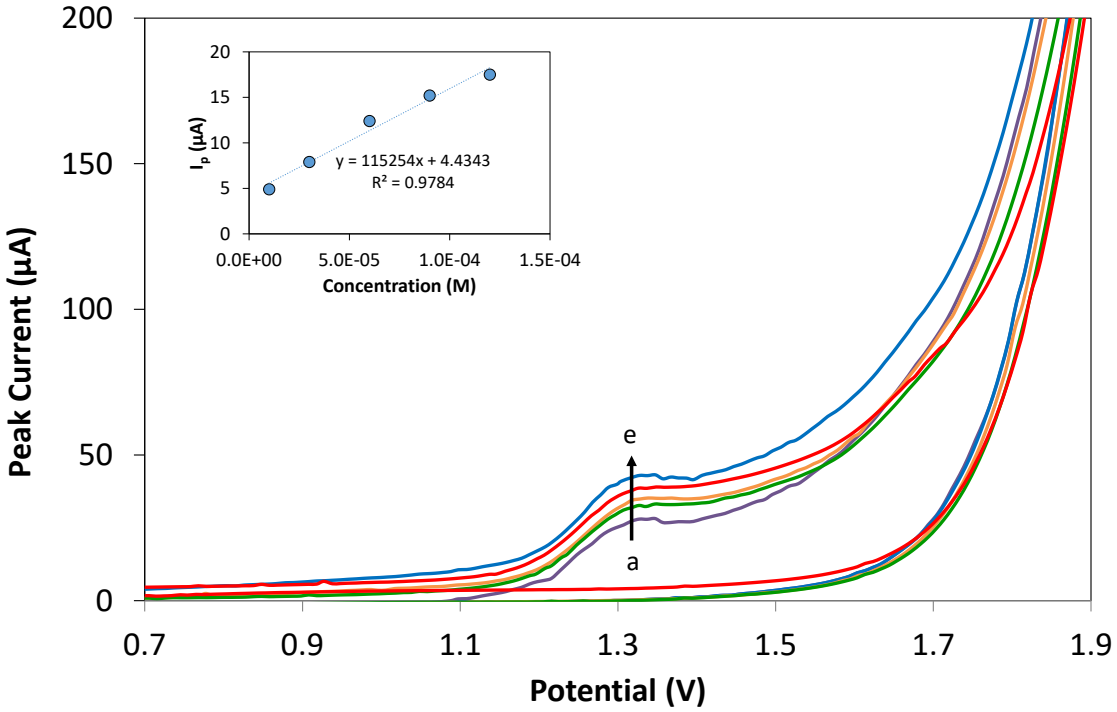
Peak Current (µA)
Potential (V)
200
150
100
50
0
0.7
0.9
1.1
1.3
1.5
1.7
1.9
e
a
I_p (µA)
20
15
10
5
0
0.0E+00
5.0E-05
1.0E-04
1.5E-04
Concentration (M)
y = 115254x + 4.4343
R² = 0.9784

Figure 3

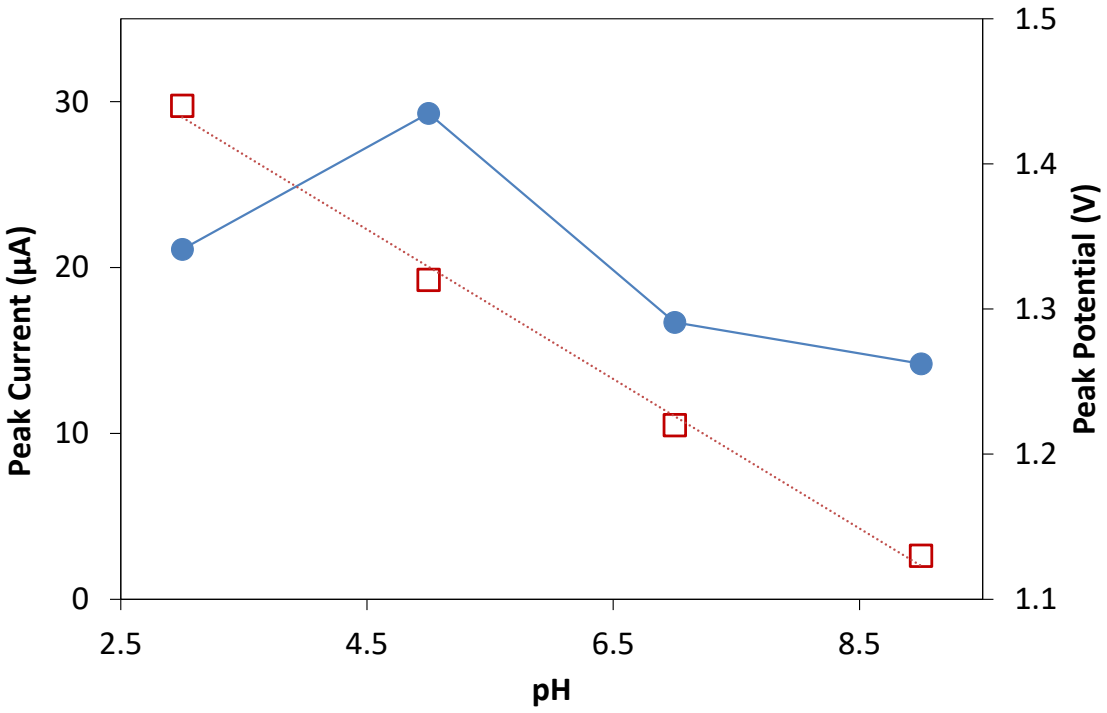
Peak Current (µA)
30
20
10
0
2.5
4.5
6.5
8.5
pH
1.5
1.4
1.3
1.2
1.1
Peak Potential (V)

Figure 4

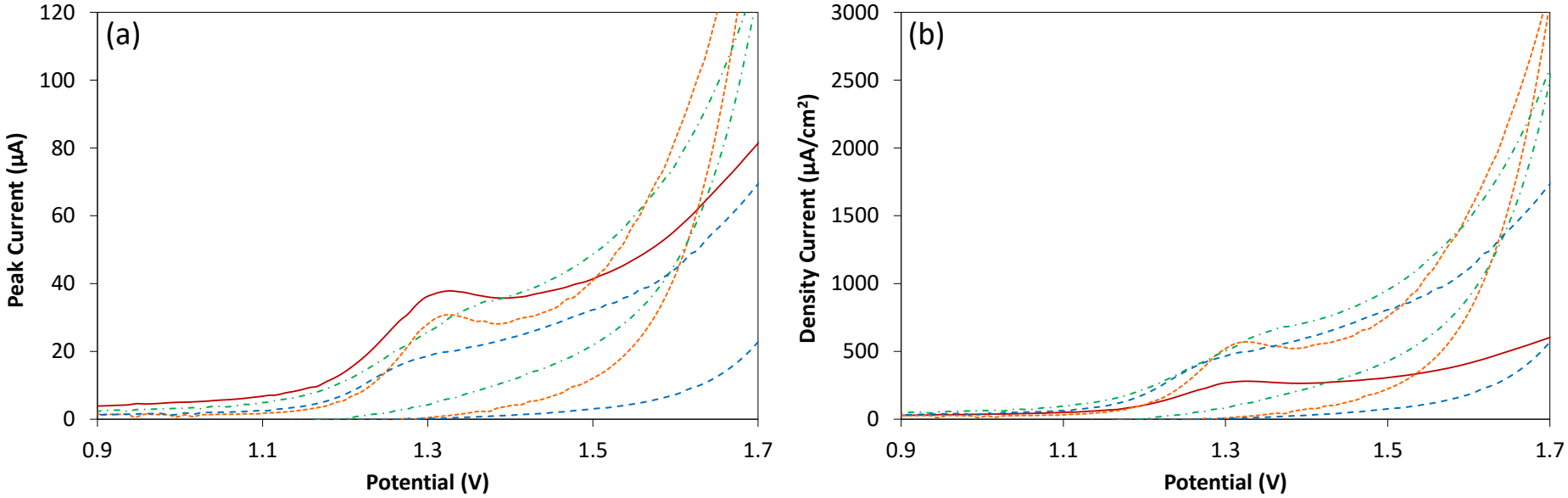
(a)
Peak Current (µA)
120
100
80
60
40
20
0
0.9
1.1
1.3
1.5
1.7
Potential (V)
(b)
Density Current (µA/cm²)
3000
2500
2000
1500
1000
500
0
0.9
1.1
1.3
1.5
1.7
Potential (V)

Figure 5

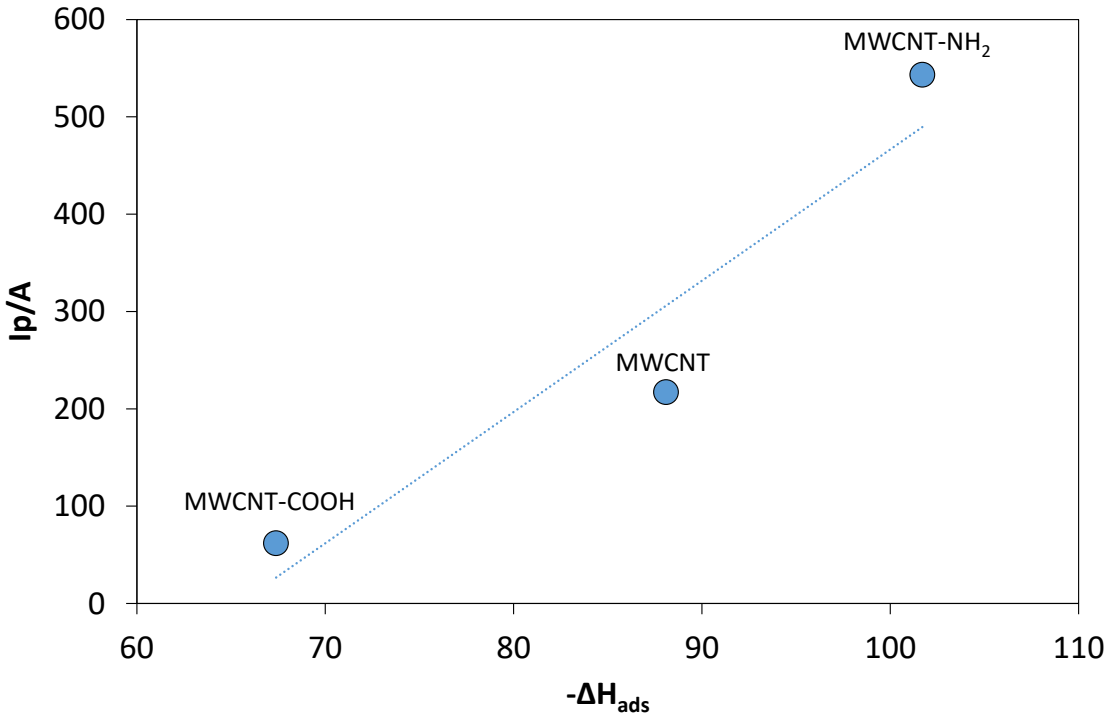
600
500
400
300
200
100
0
Ip/A
60
70
80
90
100
110
-ΔH$_{ads}$
MWCNT-NH$_2$
MWCNT
MWCNT-COOH

Figure 6

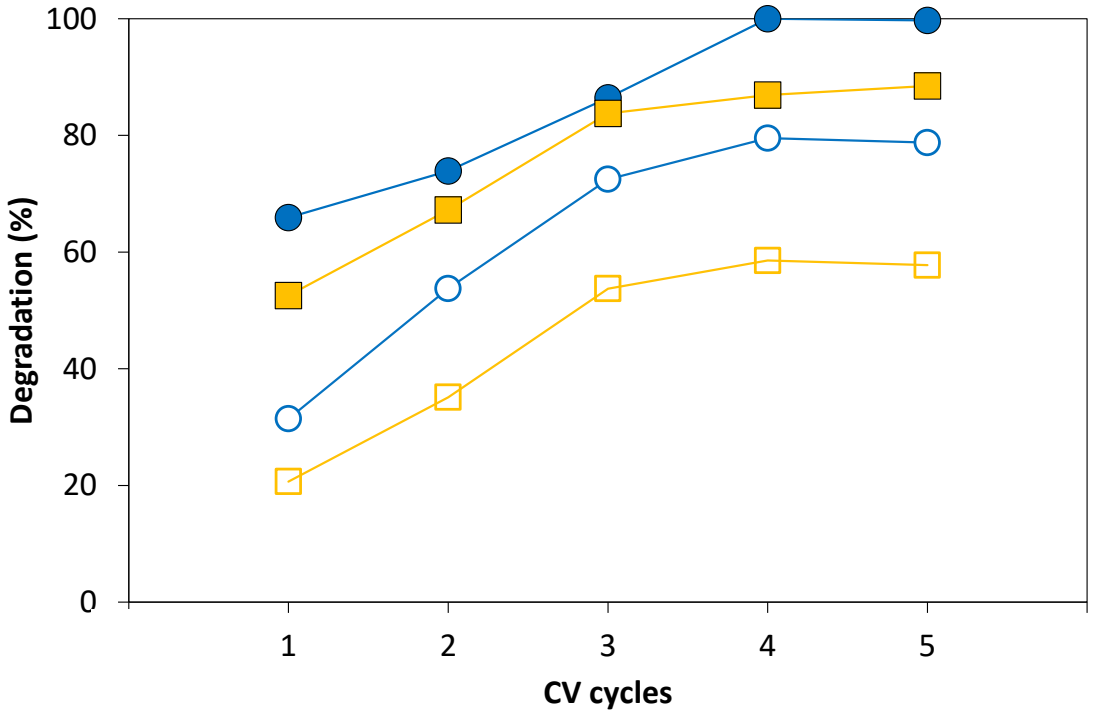

Figure 7

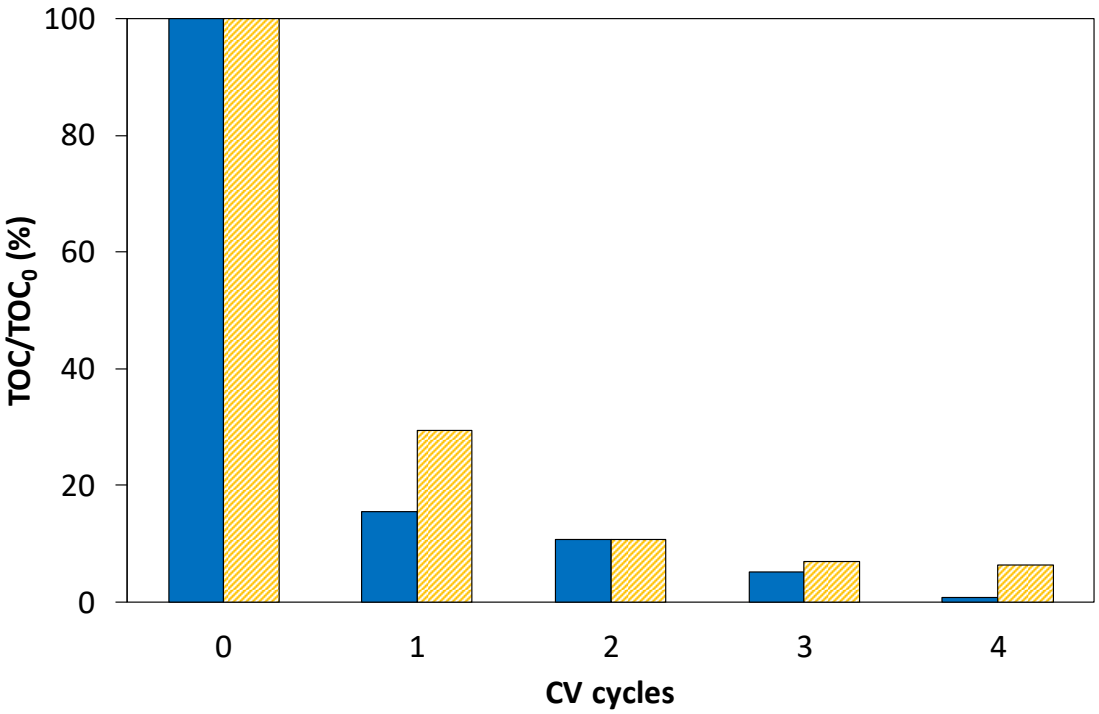

Figure 8